# Overpressure Prediction and Estimation using Eaton's and Bowers methods: Case Study of UNAG-Field, Offshore Niger Delta

[1]Unuagba, P. T, [1]Ideozu, R. U, [2]Onyekwere, R. Kelechi
[3]Oyintare Brisibe, [2]Thompson Etinosa

[1]*Department of Geology, University of Port Harcourt, Rivers State, Nigeria*
[2]*Department of Petroleum Engineering and Geosciences, Petroleum Training Institute, Effurun, Nigeria*
[3]*Department of Marine Geology, Nigeria Maritime University, Warri-South, Delta State, Nigeria*

***ABSTRACT :*** *This study is centered on overpressure detection and estimation using empirical models in UNAG-field offshore Niger Delta. Mayhems caused by overpressure in drilling operation has made overpressure studies inestimable. Eaton's and Bowers' methods have been employed to detect and estimate overpressure from sonic and density logs across three well marked as UNAG-001, 002, and 003. Three overpressure zones A, B, and C were detected in each well using the Eaton's and Bowers' 2D models with top of overpressure (TOV) at varying depths in each well. In UNAG-001, the TOVs were observed at depths of 7600ft, 9200ft, and 10,500ft. In UNAG-002, the TOVs were observed at 8100ft, 8700ft, and 10,300ft, and in UNAG-003, the TOVs were observed at 8000ft, 10,000ft, and 11,800ft. Velocity reversals from normal compaction trends were observed from sonic-velocity logs and a significant increase in pore pressure was observed away from the normal or hydrostatic pressure. Among the three overpressure zones observed, overpressure zone C has the highest magnitude of overpressure because of the abundant thick succession of shale, while the least overpressure zone was observed in zone B. Furthermore, across the wells, UNAG-001 was drilled across a more thick succession of over-pressured layers, followed by UNAG-003 and 002 respectively. Pressure estimates ranging from 4,241.25PSI to 8,471.03PSI were computed across the wells. The primary mechanism of overpressure across the wells are loading events of under compaction, although at greater depths in overpressure zone C across the three wells, unloading mechanism was responsible for the massive pressure upsurge.*

***KEYWORDS:*** *Loading and Unloading events, Overpressure, Overpressure zones, Top of overpressure*

## I. INTRODUCTION

The earth's subsurface accommodates three types of pressure which include, overburden pressure, effective stress, and formation pore pressure. While formation pore pressure acts on pore fluids, effective stress acts on the rock matrix. In addition, overburden pressure may be defined as the combination of formation pore pressure and effective stress. Formation pore pressure may be subcategorized into normal pressure, overpressure, and sub-pressure. Sub pressures are pressures below the normal formation pressure, while overpressures exceed the normal formation pressure.

Hydrocarbon bearing sequences in the Niger Delta sedimentary basin are often associated with various overpressure regimes. Deeper prospects in the Niger Delta are mostly characterized by complex substructures as a result of heavy tectonism in the zone which further increases the risks of encountering massive overpressure. It

is rare to spud an exploration well without encountering any form of formation pressure, most times trapped fluids within pore spaces in sub-formation layers are responsible for these pressures encountered.

The study of overpressure is pivotal to the success of drilling operations. In the Niger Delta, only two of the nine deep exploration wells developed by Nigeria Agip-Oil Company between 1970 and 2005 were found to be under normal pressure [1]. The wells were either abandoned, spudded without reaching the specified objective sequence, or drilled for an extended period, resulting in an exorbitant increase in drilling costs**.** Although most of the wells were drilled using the most up-to-date techniques, these issues arose [1]. Sub-optimal analysis from overpressure studies may lead to severe catastrophes like kicks, blowout, loss of drill fluid, and caving-in, all of which the drill team will aim to avoid in other to save lives, properties, drill time, and minimize environmental devastation.

Compaction-dependent geophysical wireline tools like density, sonic, and resistivity logs act as a proxy to overpressure, thus overpressure analysis is centered on them [2]. Overpressure could be predicted and estimated in three ways which are, predrill, postdrill, and while drilling methods respectively. Each of these methods has its uniqueness in detecting overpressure play in the sub formation. Predrill methods analyses the sub formation pressure play before drilling activity commences, a typical predrill method is the seismic approach. Post drill method encompasses all studies carried out on already spudded wildcat wells and available seismic data to drill new exploration, appraisal, or production wells. Furthermore, while drilling methods are live geophysical measurements carried in the course of drilling.

Overpressure in sedimentary basin sub-formations has been attributed to a host of pressure mechanisms. These mechanisms are responsible for overpressure build-up in the sub formations, however, it varies from basin to basin due to rock formation complexities [3]. Loading and unloading mechanisms have been the two most prevalent overpressure mechanisms in the subsurface of the Niger Delta Basin. In events of rapid deposition and burial of sediments, pore fluids in the formation may not be properly expelled due to rapid compaction induced by the weight of the overlying deposited sediments, thus these partially expelled fluids are trapped in the under-compacted subsurface and may be subjected to overpressure if loading (continuous deposition) of sediments remains constant, this scenario is called disequilibrium compaction or under-compaction. Furthermore, unloading mechanism of overpressure may occur at the precipice of loading events or when a geologic event abruptly stops the mechanical process of compaction, thereby reducing density at that depth. Tectonic, fluid expansion, illitization and thermal cracking of hydrocarbon have been attributed to be some of the key culprits that induces unloading.

Sedimentary layers associated with overpressure have distinct characteristic properties when compared to normally pressured layers at the same depth, these overpressure layers may exhibit high porosity, high Poisson Ratio, low compressional velocity, and bulk density respectively [4, 5]. Like formation pressure, compressional velocity, bulk density, and resistivity increases with depth, however, overpressure scenarios could be observed as any significant deflection away from the normal travel trend in depth in the aforementioned geophysical wireline tools.

Overpressure detection techniques now in use take advantage of deviations in formation properties from an expected or typical trend in the area of interest. Well logs are the most widely used and trustworthy method for constructing trends and detecting overpressures. This detection trend has birthed a host of empirical models that aided geoscientists to accurately detect and estimate overpressure. In his mathematical expression, Terzaghi [6], formulated a simple compaction equation that related overburden pressure as the summation of effective stress and formation pore pressure. From this premise, Eaton [7] and Bowers [8] modified Terzaghi's empirical model by incorporating well log parameters to detect and estimate overpressure. While Eaton's empirical relation has been relatively prominent among geoscientists in overpressure detection, Bowers method has been modified to account for overpressure triggered by loading and unloading events by analyzing the effective stress relationship with depth in the formation. This study is centered on using Eaton's and Bowers' empirical models to detect and estimate overpressure. Bowers empirical method has been employed specifically to formation depths associated with overpressure from unloading source.

## II. GEOLOGICAL SETTING OF THE STUDY AREA

The Niger Delta sedimentary basin is situated in the Gulf of Guinea and represents the southernmost end of the extensive intracontinental Benue Trough. The geology of the sedimentary basin has been split into onshore and offshore provinces respectively. The Northern margins of the onshore province transect the Anambra basin which has been seen as an extension of the intracontinental Benue trough, while the western and southern margins have been bounded by the Dahomey basin and Calabar flank. Furthermore, the Niger Delta offshore province is delineated by the Cameroon volcanic line in the east as well as the Dahomey basin in the west. The delta has prograded southwestward from Eocene to Recent, generating depobelts that represent the delta's most active part at each stage of development [9]. With a surface area of 300,000 km$^2$ [10], a sediment volume of 500,000 km$^3$ [11], and a sediment thickness of more than 10 km [12] in the basin depocenter, these depobelts comprise one of the world's greatest regressive deltas. The Niger Delta stratigraphic sequence is made up of three lithostratigraphic units identified as, the Akata, Agbada, and Benin Formations, which are all extremely diachronous and are arranged from oldest to youngest [13].

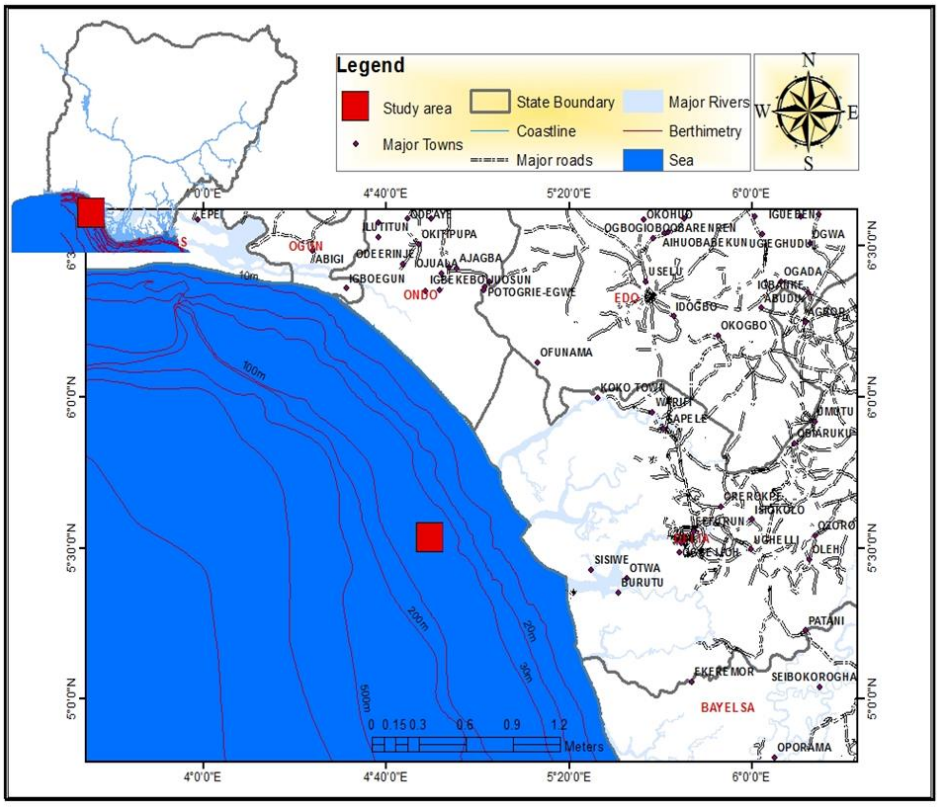


**Fig 1.** Location map of the study area

## III. METHODOLOGY

The data set utilized in this study includes sonic-velocity and density logs from three wells namely, UNAG-001, 002 and 003. This study is limited to post-drill overpressure detection and estimation methods, based on the available data. The data was analysed using the Rokdoc and Microsoft Excel software tools.

**Pore pressure estimation method**

Terzaghi's [6], Eaton's [7] and Bowers [8], empirical relations have been used to estimate the overpressures predicted from effective stress and compressional velocity in this study. Eaton's method is a widely accepted empirical method for pressure estimation that analyzes resistivity/sonic velocity data by comparing in-

situ physical properties (resistivity or velocity) to normally compacted equivalent physical properties at the same depth. Bowers empirical method accounts for the case of overpressures caused by unloading mechanisms that are not alien to the Niger Delta formation. Unloading intervals are zones of (effective) stress hysteresis in which the effective stress reduces and is maintained at a low level without any significant increase in porosity or reduced density from density logs [3].

**Terzaghi overburden stress determination (Terzaghi [6])**

Conventional methods of overpressure estimation stem from the theory of compaction which relates pore pressure with the physical properties of a formation and this fundamental assumption is based on Terzaghi's original relation which analyses compaction caused by overburden stress, as shown in Eqn. 1.

$$\sigma V = \sigma e + P \quad (1)$$

Where overburden stress - (**σ**v), pore pressure - (P), and effective stress - (**σ**e). The relationships between these pressures are shown in Fig. 2. Based on this assumption, many empirical methods which estimate overpressure was founded. By rearranging Terzaghi's equation, it is possible to calculate the overpressure in shales if the overburden and effective stress are known/estimated from Eqn. 2;

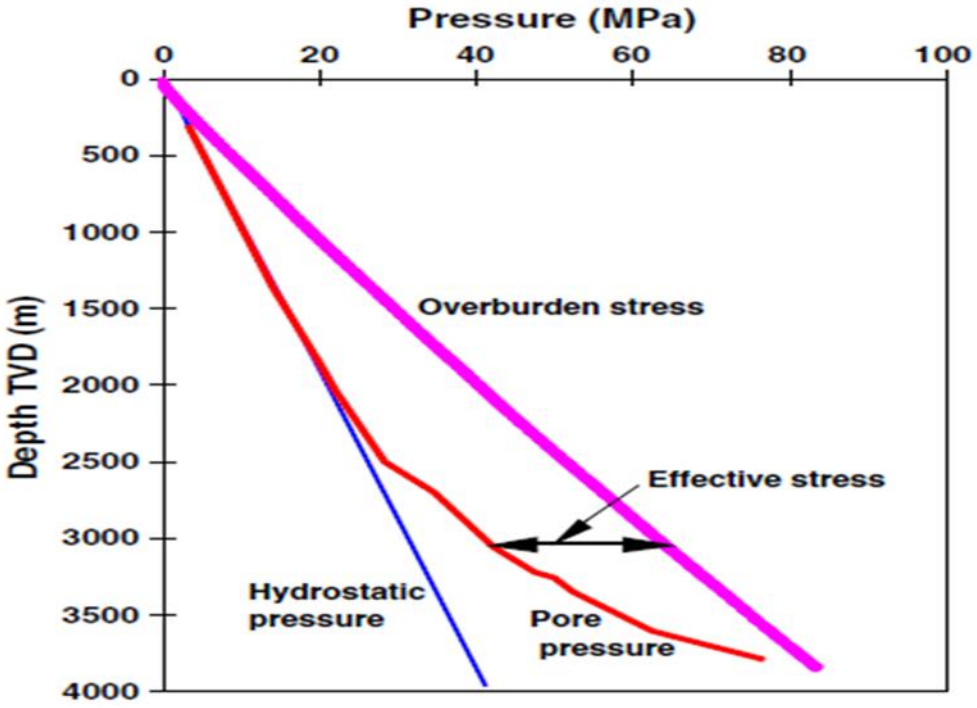


**Fig 2.** A schematic representation of different pressures and their relationships in a borehole (modified after [13]).

$$\sigma V - \sigma e = P \quad (2)$$

Where $\sigma V$ – overburden stress, $\sigma e$ – effective stress, $P$ – pore pressure.

The overburden stress can also be calculated directly from density log data.

**Eaton's transit time method**

Eaton [7], devised an approach for relating acoustic velocity to formation pore pressure in well logs. The following is a derivative of Eaton's method used and applied in this research;

From Terzaghi's relation in Eqn. (2) Eaton deduced;

$$P = \sigma V - \sigma e \quad (3)$$

Thereafter, the established relationship between sonic log and measured pressure data in clean shale from Terzaghi is given as;

$$P = \Delta to - \Delta tn \quad (4)$$

Where $\Delta to$ = observed sonic transit time in shale and $\Delta tn$ = normal transit travel time in shale, since log parameters are a function of P, **σ**v, and **σ**e respectively,

$$P = \sigma V - \sigma e \left[\frac{\Delta tn}{\Delta to}\right]^{3.0} \quad (5)$$

Eaton developed an empirical relationship that predicted overpressure behaviour with effective stress constant given as;

$$P = \sigma V - 0.535 \left[\frac{\Delta tn}{\Delta to}\right]^{3.0} \quad (6)$$

From equation (6), **σ**e = 0.535 (effective stress constant/gradient), If overburden pressure (**σ**v) and change in transit time in the formation (transit time ratio [Δtn/Δto]) = 1, the formation will be normally pressured (Pn).

$$Pn = 1 - 0.535(1.0)^{3.0} = 0.465\text{psi/ft} \quad (7)$$

0.465psi/ft = normal pressure gradient for salt water

Rearranging Eqn.3 to express effective stress in normal geo-pressure situation the formula can be expressed thus;

$$\sigma e = \sigma V - Pn \quad (8)$$

However, equation (6) shows that in abnormal geo-pressure situations, the effective stress is approximately;

$$\sigma e = 0.535 \left[\frac{\Delta tn}{\Delta to}\right]^{3.0} \quad (9)$$

Thus, Eqn.9 represents effective stress ($\sigma e$) when there is an abnormal change in transit travel time which proves; $\sigma e = 0.535$ (effective stress constant in normal pressured events) when

$Pn = 0.465\ psi/ft$ and

$\left[\frac{\Delta tn}{\Delta to}\right]^{3.0} = 1.$

If the right-hand side of Eqn.8 is substituted into Eqn.9, effective stress can be directly related to acoustic values of clean shale as follow;

$$\sigma e = \sigma v - Pn \left[\frac{\Delta tn}{\Delta to}\right]^{3.0} \quad (10)$$

Eqn. (3) shows that abnormal pore pressure prediction is a function of the difference of overburden pressure and effective stress but in Eqn. 9 effective stress ($\sigma e$) functions as a proxy for prediction of formation pore pressure because, effective stress ($\sigma e$) is directly proportional to the overburden weight (as overburden increases, effective stress increases) but if the effective stress is abnormally low when the weight of overburden is high at a particular depth, it therefore indicates overpressure, thus, in this scenario, Pore pressure can be estimated with Eqn.3 – if the overburden and effective stresses are known, and Eqn.10 – because effective stress magnitude is inversely proportional to pore pressure (low effective stress results to overpressure vice versa).

However, Eaton combined the aforementioned equations to account for the estimation of both normal and overpressure conditions by substituting Eqn.10 into Eqn.3 which was employed in this study.

$$p = \sigma V - (\sigma V - Pn) \left[\frac{\Delta tn}{\Delta to}\right]^{3.0} \quad (11)$$

**Bowers method**

Overpressure was predicted from Bowers [8] empirical relation modified to account for sonic log parameters expressed as;

$$P = \boldsymbol{\sigma}\text{v} - \left(\frac{(Vp - Vml)}{A}\right)^{\frac{1}{B}} \quad (12)$$

Where $Vp$ = compressional velocity at any depth, $Vml$ = mudline compressional velocity, $\sigma e$ = effective stress, A and B = calibrated parameters with the offset velocity versus effective stress ($\sigma e$).

However, a modified Bowe relation which accounts for sonic transit time by replacing $10^6/\Delta t$ for Vp and $10^6/\Delta tml$ for $V_{ml}$ in Eqn.12 was employed to evaluate overpressure from sonic log;

$$P = \sigma v - \left(\frac{10^{6\left(\frac{1}{\Delta t}-\frac{1}{\Delta tml}\right)}}{A}\right)^{\frac{1}{B}} \quad (13)$$

Where $\Delta t_{ml}$ is the mudline $V_p$ transit time, normally $\Delta tml$ =200 µs/ft or 660 µs/m.

When unloading occurs, compressional velocity (Vp) and effective stress do not follow the normal loading curve, and according to Bowers [2], a higher velocity than the velocity in the loading curve will appear at the same effective stress in the event of unloading thus, Bowers [8],published the following equation to account for unloading:

$$Vp = Vml + A\left[\sigma \max\left(\frac{\sigma e}{\sigma max}\right)^{\frac{1}{u}}\right]^{B} \quad (14)$$

Where σe, Vp, Vml, A and B still represent their aforementioned parameters, "U" represents the uplift parameter (unloading); and

$$\sigma \max = \left(\frac{Vmax - Vml}{A}\right)^{\frac{1}{B}} \quad (15)$$

Where $\sigma max$ and $Vml$ represent estimates of effective stress and velocity at the inception of unloading. In absence of major lithological changes, $V_{max}$ is usually calibrated to equal the velocity at the onset of the velocity reversal.

Rearranging Eqn.14 overpressure can be calculated from the unloading event with the following equation;

$$Pulo = \sigma v - \left(\frac{vp - vml}{A}\right)^{\frac{U}{B}} (\sigma \max)^{1-U} \quad (16)$$

*Where Pulo* is the unloading interval overpressure.

## IV. RESULTS AND DISCUSSION

The results obtained in this study are shown in Figures 3 – 6 and Tables 1 – 12. The 2D models of overpressure estimates were generated for the three wells (UNAG-001, 002 and 003) in Figure 4. Significant depth intervals for these wells ranges from 4000ft – 12500ft, with UNAG-003 the deepest (5000ft – 12500ft), followed by UNAG-001 (6000ft – 12000ft) and UNAG-002 (4000ft – 11000ft). Across the wells, three overpressure zones have been identified, the zones are categorized as Overpressure Zones A, B, and C respectively. In Figure 3, the top of the overpressured zones (TOV) A, B, and C for UNAG-001 has been identified at 7600ft, 9200ft, and 10500ft respectively, while for UNAG-002, the top of overpressure was identified at 81000ft, 8700ft, and 10300ft. In UNAG-003, 8000ft, 10000ft, and 11800ft were the respective tops of overpressure zones.

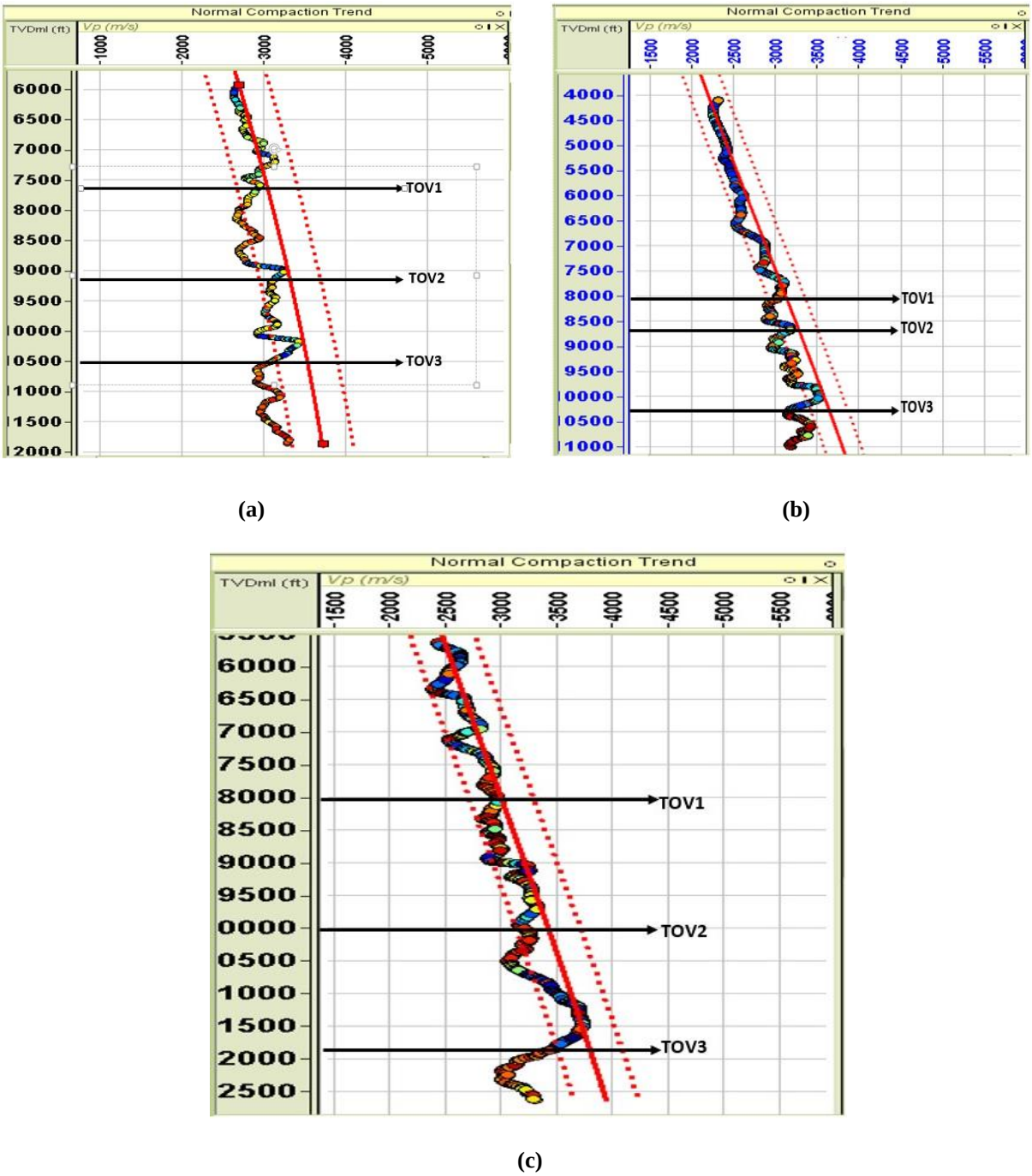


**Fig 3.** Top of Overpressure identified from velocity normal compaction trend for the three wells.

Furthermore, the terminal depth of overpressure of these overpressure zones across the wells include, 8800ft, 10100ft, 11000ft for UNAG-001, 8500ft, 9700ft, 11000ft for UNAG-002 and, 9000ft, 10500ft, 12500ft for UNAG-003. The overpressure zones vary in depth thickness from well to well, in UNAG-001, the respective thicknesses of the three identified overpressure zones A, B and C are, 1200ft, 900ft, and 500ft. For UNAG-002, the depth thickness of the overpressure zones is 400ft, 1000ft, and 700ft, while for UNAG-003, overpressure zones A, B, and C have been Identified to be 1000ft, 500ft, and 700ft thick. Pore pressure estimates for the three wells have been recorded in Tables 1 – 3. Furthermore, the pressure readings were subdivided to isolate only overpressure readings from the mapped out overpressure zones across the wells, see Tables 3 – 12. Table 13 contains the general overview of the pressure play in all the overpressure zone across the wells. Figures 5 – 6

contains scattered plot chart showing the correlations of all the overpressure magnitude between these over pressured zones in each of the wells.

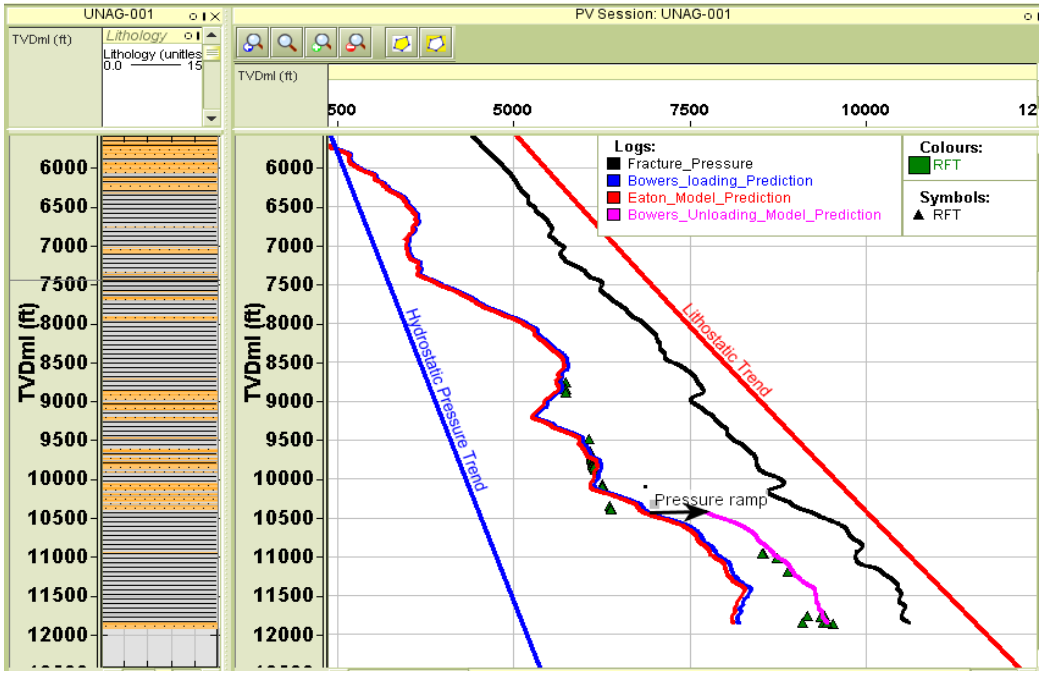


**(a)**

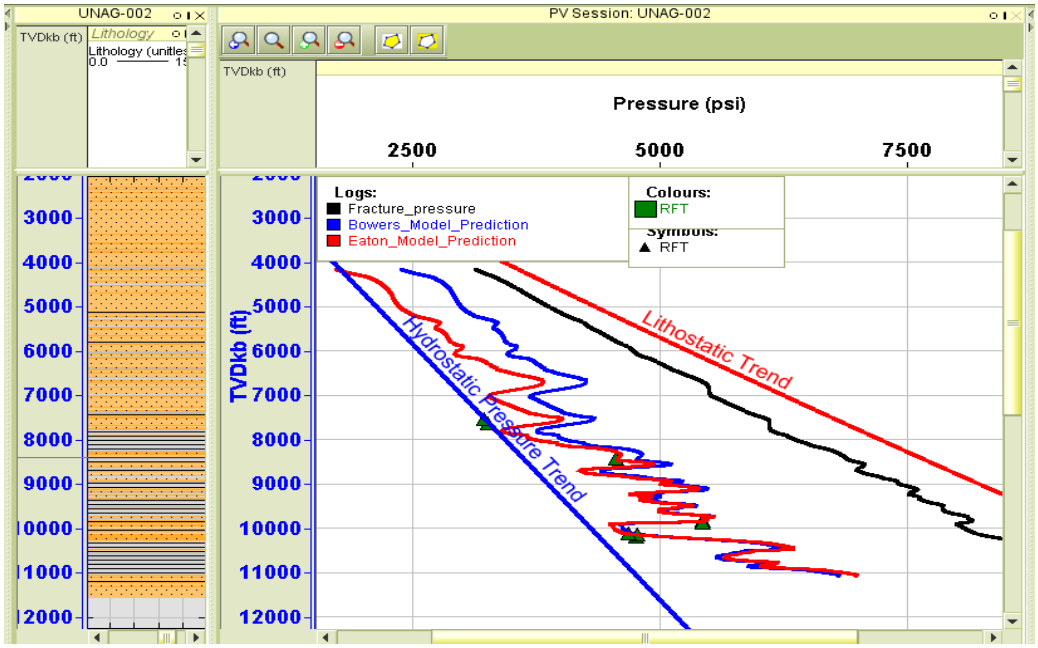


**(b)**

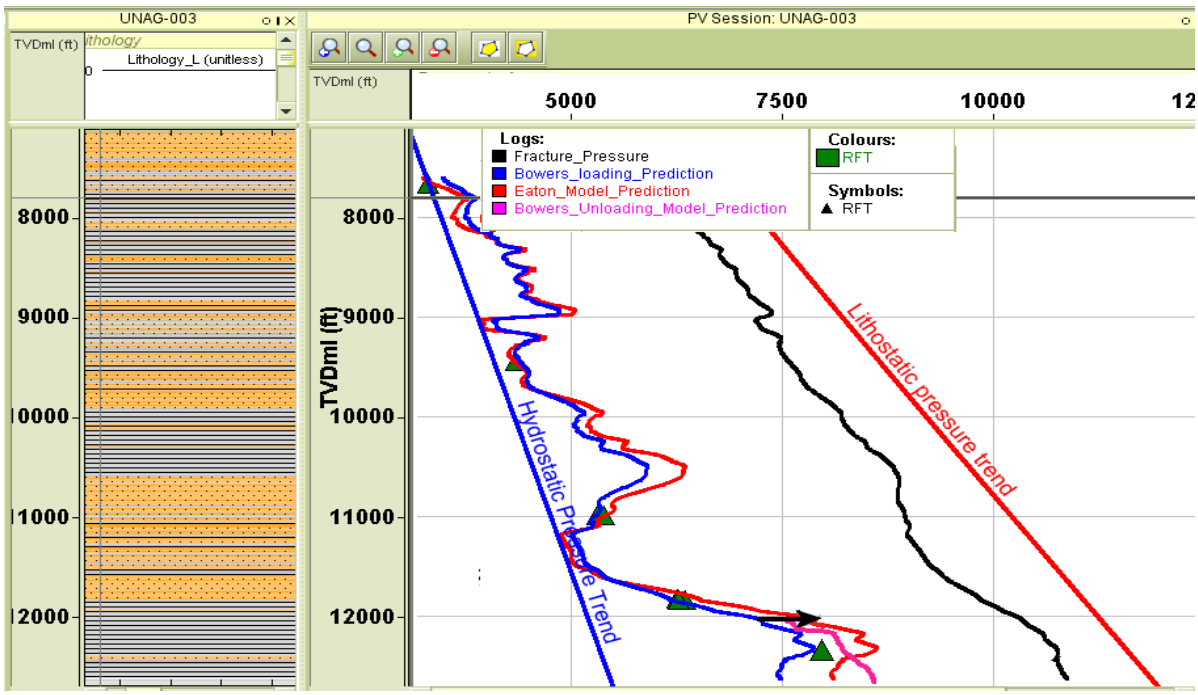


**(c)**

**Fig 4 (a, b, c).** Eaton's and Bowers empirical models showing estimates of overpressures in UNAG-001, 002 and 003 wells.

**Table 1: Summary of Overpressure values estimated for UNAG-001**

| | Overpressure values estimated from Eaton's and Bowers Empirical method for UNAG-001 well | | | | |
|---|---|---|---|---|---|
| **S/N** | **Significant depth (ft)** | **Normal pressure (psi)** | **Eaton's estimated overpressure (psi)** | **Bowers Estimated overpressure (psi)** | **Bowers unloading overpressure (psi)** |
| 1 | 6000 | 2594.6 | 2635.1 | 2702.7 | |
| 2 | 6100 | 2648.6 | 3067.6 | 3108.1 | |
| 3 | 6200 | 2689.2 | 3121.6 | 3175.7 | |
| 4 | 6300 | 2729.7 | 4243.2 | 3310.8 | |
| 5 | 6400 | 2770.3 | 3445.9 | 3513.5 | |
| 6 | 6500 | 2837.8 | 3527 | 3621.6 | |
| 7 | 6600 | 2878.4 | 3599.3 | 3675.7 | |
| 8 | 6700 | 2905.4 | 3581.1 | 3648.6 | |
| 9 | 6800 | 2945.9 | 3501.4 | 3567.6 | |

| | | | | |
|---|---|---|---|---|
| 10 | 6900 | 2999.9 | 3472.9 | 3527 |
| 11 | 7000 | 3040.5 | 3486.5 | 3554.1 |
| 12 | 7100 | 3094 | 3499.9 | 3567.6 |
| 13 | 7200 | 3121.6 | 3594.6 | 3648.6 |
| 14 | 7300 | 3162.2 | 3648.6 | 3716.2 |
| 15 | 7400 | 3216.2 | 3729.7 | 3783.8 |
| 16 | 7500 | 3256.8 | 4054.1 | 4108.1 |
| 17 | 7600 | 3297.3 | 4121.6 | 4189.2 |
| 18 | 7700 | 3310.8 | 4395.9 | 4472.9 |
| 19 | 7800 | 3364.8 | 4594.6 | 4662.2 |
| 20 | 7900 | 3432.4 | 4837.8 | 4938.4 |
| 21 | 8000 | 3540.5 | 5189.2 | 5270.3 |
| 22 | 8100 | 3527 | 5337.8 | 5391.9 |
| 23 | 8200 | 3554.1 | 5391.9 | 5472.9 |
| 24 | 8300 | 3585.1 | 5472.9 | 5540.5 |
| 25 | 8400 | 3635.1 | 5662.2 | 5743.2 |
| 26 | 8500 | 3689.2 | 5675.7 | 5747.3 |
| 27 | 8600 | 3743.2 | 5608.1 | 5675.7 |
| 28 | 8700 | 3770.2 | 5567.6 | 3648.6 |
| 29 | 8800 | 3824.3 | 5540.5 | 5581.1 |
| 30 | 8900 | 3864.9 | 5540.5 | 5540.5 |
| 31 | 9000 | 3918.9 | 5405.4 | 5405.4 |
| 32 | 9100 | 3959.5 | 5351.4 | 5351.4 |
| 33 | 9200 | 3986.5 | 5405.4 | 5472.9 |
| 34 | 9300 | 4027 | 5472.9 | 5527 |
| 35 | 9400 | 4067.6 | 5770.3 | 5810.8 |
| 36 | 9500 | 4121.6 | 6081.1 | 6148.6 |
| 37 | 9600 | 4162.2 | 6083.8 | 6216.2 |
| 38 | 9700 | 4229.7 | 6175.7 | 6229.7 |

| | | | | | |
|---|---|---|---|---|---|
| 39 | 9800 | 4256.8 | 6149.9 | 6216.2 | |
| 40 | 9900 | 4324.3 | 6145.1 | 6202.7 | |
| 41 | 10000 | 4364.9 | 6094.6 | 6151.4 | |
| 42 | 10100 | 4405.4 | 6094.6 | 6148.6 | |
| 43 | 10200 | 4445.9 | 6081.1 | 6135.1 | |
| 44 | 10300 | 4486.5 | 6486.5 | 6540.5 | |
| 45 | 10400 | 4513.5 | 6759.8 | 6824.3 | 7770.3 |
| 46 | 10500 | 4540 | 7162.2 | 7229.7 | 8162.2 |
| 47 | 10600 | 4594.6 | 7432.4 | 7499.9 | 8216.2 |
| 48 | 10700 | 4662.2 | 7621.6 | 7702.7 | 8472.9 |
| 49 | 10800 | 4716.2 | 7743.2 | 7824.3 | 8540.5 |
| 50 | 10900 | 4770.2 | 7810.8 | 7905.4 | 8648.6 |
| 51 | 11000 | 4797.3 | 7891.9 | 7972.9 | 8785.8 |

**Table 2: Summary of Overpressure values estimated for UNAG-002**

| Overpressure values estimated from Eaton's and Bowers Empirical method for UNAG-002 well | | | | | |
|---|---|---|---|---|---|
| **S/N** | **Significant depth (ft)** | **Normal pressure (psi)** | **Eaton's estimated overpressure (psi)** | **Bowers Estimated overpressure (psi)** | **Bowers unloading overpressure (psi)** |
| 1 | 4200 | 1798.1 | 1807.7 | 2355.8 | |
| 2 | 4300 | 1836.5 | 2019.3 | 2634.6 | |
| 3 | 4400 | 1875 | 2163.5 | 2884.6 | |
| 4 | 4500 | 1932.7 | 2211.5 | 2932.7 | |
| 5 | 4600 | 1980.7 | 2235.4 | 2942.3 | |
| 6 | 4700 | 2009.6 | 2307.7 | 2951.9 | |
| 7 | 4800 | 2067.3 | 2317.3 | 2961.5 | |
| 8 | 4900 | 2105.8 | 2355.4 | 2980.8 | |
| 9 | 5000 | 2163.5 | 2403.9 | 3008.6 | |
| 10 | 5100 | 2211.5 | 2451.9 | 3076.9 | |
| 11 | 5200 | 2259.6 | 2301 | 3125 | |

| | | | | |
|---|---|---|---|---|
| 12 | 5300 | 2307.7 | 2788.5 | 3365.4 |
| 13 | 5400 | 2355.8 | 2836.5 | 3413.5 |
| 14 | 5500 | 3494.3 | 2849.5 | 3432.7 |
| 15 | 5600 | 2423.1 | 2875 | 3442.3 |
| 16 | 5700 | 2480.8 | 2884.6 | 3451.9 |
| 17 | 5800 | 2500 | 2894.2 | 3461.5 |
| 18 | 5900 | 2548.1 | 2932.7 | 3490.4 |
| 19 | 6000 | 2596.2 | 2913.5 | 3471.2 |
| 20 | 6100 | 2644.2 | 2903.8 | 3442.3 |
| 21 | 6200 | 2682.7 | 3173.1 | 3750 |
| 22 | 6300 | 2730.8 | 3365.4 | 3846.2 |
| 23 | 6400 | 2788.5 | 3375 | 3903.8 |
| 24 | 6500 | 2836.5 | 3461.5 | 4086.5 |
| 25 | 6600 | 2865.4 | 3653.8 | 4105.8 |
| 26 | 6700 | 2894.2 | 3798.1 | 4230.8 |
| 27 | 6800 | 2923.1 | 3653.8 | 4038.5 |
| 28 | 6900 | 2971.2 | 3557.7 | 3942.3 |
| 29 | 7000 | 3009.6 | 3269.3 | 3682.7 |
| 30 | 7100 | 3067.3 | 3365.4 | 3759.6 |
| 31 | 7200 | 3105.8 | 3500 | 3894.2 |
| 32 | 7300 | 3163.5 | 3557.7 | 3942.3 |
| 33 | 7400 | 3182.7 | 3653.8 | 4086.5 |
| 34 | 7500 | 3221.2 | 4038.5 | 4326.9 |
| 35 | 7600 | 3240.4 | 3942.3 | 4270.8 |
| 36 | 7700 | 3259.6 | 3750 | 4038.5 |
| 37 | 7800 | 3278.8 | 3596.2 | 3942.3 |
| 38 | 7900 | 3336.5 | 3336.5 | 3750 |
| 39 | 8000 | 3413.5 | 3798.1 | 4134.6 |
| 40 | 8100 | 3538 | 3942.3 | 4038.5 |

| | | | | |
|---|---|---|---|---|
| 41 | 8200 | 3367.3 | 4230.8 | 4278.8 |
| 42 | 8300 | 3605.9 | 4519.2 | 4711.5 |
| 43 | 8400 | 3644.4 | 4567.3 | 4807.7 |
| 44 | 8500 | 3653.8 | 4615.4 | 4807.7 |
| 45 | 8600 | 3711.5 | 4619.2 | 4567.3 |
| 46 | 8700 | 3750 | 4500 | 4548.1 |
| 47 | 8800 | 3788.5 | 4423.1 | 4519.2 |
| 48 | 8900 | 3826.9 | 4625 | 4663.5 |
| 49 | 9000 | 3884.6 | 5000 | 5048.1 |
| 50 | 9100 | 3923.1 | 5192.3 | 5288.5 |
| 51 | 9200 | 3971.2 | 4711.5 | 4903.9 |
| 52 | 9300 | 3971.2 | 4915.4 | 5000 |
| 53 | 9400 | 4048.1 | 4998.1 | 5049 |
| 54 | 9500 | 4096.2 | 5192.3 | 5240.4 |
| 55 | 9600 | 4134.6 | 5028.7 | 5050.9 |
| 56 | 9700 | 4182.7 | 5480.8 | 5528.8 |
| 57 | 9800 | 4240.4 | 5480.8 | 5500 |
| 58 | 9900 | 4278.8 | 4451.9 | 4471.1 |
| 59 | 10000 | 4326.9 | 4519.2 | 4615.4 |
| 60 | 10100 | 4375 | 4663.5 | 4711.5 |
| 61 | 10200 | 4403.8 | 4711.5 | 4807.4 |
| 62 | 10300 | 4451.9 | 5673.1 | 5676.6 |
| 63 | 10400 | 4500 | 6355.8 | 6346.2 |
| 64 | 10500 | 4548.1 | 5961 | 5942.3 |
| 65 | 10600 | 4586.6 | 5673.1 | 5579.9 |
| 66 | 10700 | 4615.4 | 5663.5 | 5557.7 |
| 67 | 10800 | 4663.5 | 5965.4 | 5971.2 |
| 68 | 10900 | 4711.5 | 6057.8 | 5865.4 |
| 69 | 11000 | 4758.6 | 6923.1 | 6826.9 |

**Table 3: Summary of Overpressure values estimated for UNAG-003**

| | Overpressure values estimated from Eaton's and Bowers Empirical method for UNAG-003 well | | | | |
|---|---|---|---|---|---|
| **S/N** | **Significant depth (ft)** | **Normal pressure (psi)** | **Eaton's estimated overpressure (psi)** | **Bowers Estimated overpressure (psi)** | **Bowers unloading overpressure (psi)** |
| 1 | 7600 | 3308.8 | 3529.4 | 3602.9 | |
| 2 | 7700 | 3352.9 | 3676.5 | 3823.5 | |
| 3 | 7800 | 3382.3 | 3548.1 | 3724.9 | |
| 4 | 7900 | 3426.5 | 3676.5 | 3823.5 | |
| 5 | 8000 | 3455.9 | 3576.5 | 3676.5 | |
| 6 | 8100 | 3529.4 | 3695 | 3823.5 | |
| 7 | 8200 | 3573.5 | 4117.6 | 4147 | |
| 8 | 8300 | 3647.1 | 4411.8 | 4470.6 | |
| 9 | 8400 | 3676.5 | 4264.7 | 4308.8 | |
| 10 | 8500 | 3705.9 | 4382.3 | 4411.8 | |
| 11 | 8600 | 3749.9 | 4558.8 | 4573.5 | |
| 12 | 8700 | 3794.1 | 4411.8 | 4455.9 | |
| 13 | 8800 | 3838.2 | 4485.3 | 4544.1 | |
| 14 | 8900 | 3897.1 | 4705.9 | 4779.4 | |
| 15 | 9000 | 3941.2 | 4044.1 | 4117.6 | |
| 16 | 9100 | 3970.6 | 3999.9 | 4117.6 | |
| 17 | 9200 | 4014.7 | 4151 | 4264 | |
| 18 | 9300 | 4058 | 4485.2 | 4558.8 | |
| 19 | 9400 | 4102.9 | 4264.7 | 4338.2 | |
| 20 | 9500 | 4147 | 4441.2 | 4544.1 | |
| 21 | 9600 | 4235.3 | 4485.3 | 4558.8 | |
| 22 | 9700 | 4264.7 | 4852.9 | 4882.3 | |
| 23 | 9800 | 4279.4 | 5000 | 5147.1 | |
| 24 | 9900 | 4294.1 | 5073.5 | 5294.1 | |

| | | | | | |
|---|---|---|---|---|---|
| 25 | 10000 | 4294.1 | 5102.9 | 5338.2 | |
| 26 | 10100 | 4323.5 | 5073.5 | 5235.3 | |
| 27 | 10200 | 4411.8 | 5279.4 | 5294.1 | |
| 28 | 10300 | 4470.6 | 5367.6 | 5632.3 | |
| 29 | 10400 | 4518.7 | 5808.8 | 6220.6 | |
| 30 | 10500 | 4558.8 | 5882.3 | 6323.5 | |
| 31 | 10600 | 4632.3 | 5735.3 | 6045.6 | |
| 32 | 10700 | 4676.5 | 5588.3 | 5882.3 | |
| 33 | 10800 | 4705.9 | 5367.6 | 5529.4 | |
| 34 | 10900 | 4749.9 | 5308.8 | 5499.9 | |
| 35 | 11000 | 4823.5 | 5264.7 | 5308.8 | |
| 36 | 11100 | 4852.9 | 5308.8 | 5323.5 | |
| 37 | 11200 | 4882.3 | 4882.3 | 5073.5 | |
| 38 | 11300 | 4926.5 | 4941.2 | 5147.1 | |
| 39 | 11400 | 4999.9 | 5000 | 5177.9 | |
| 40 | 11500 | 5029.4 | 5166.2 | 5294.1 | |
| 41 | 11600 | 5073.5 | 5279.4 | 5073.5 | |
| 42 | 11700 | 5117.6 | 5441.2 | 5117.6 | |
| 43 | 11800 | 5147.1 | 6470.6 | 6176.5 | |
| 44 | 11900 | 5205.9 | 6617.6 | 6323.5 | |
| 45 | 12000 | 5264.7 | 7794.1 | 7205.8 | 7500.3 |
| 46 | 12100 | 5279.4 | 8088.2 | 7352.9 | 7647.1 |
| 47 | 12200 | 5352.9 | 8529.4 | 7779.4 | 7838.2 |
| 48 | 12300 | 5382.4 | 8676.5 | 7926.5 | 8220.6 |
| 49 | 12400 | 5411.8 | 8382.3 | 7794.1 | 8352.9 |
| 50 | 12500 | 5429.5 | 8235.3 | 7500.1 | 8485.3 |
| 51 | 12600 | 5441.2 | 8088.3 | 7514.7 | 8602.9 |
| 52 | 12700 | 5470.6 | 8117.6 | 7470.6 | 8661.8 |

**Table 4: Overpressure values estimated from Eaton's and Bowers method in overpressure zone A, Unag 001 well (TOV at 7600ft)**

| Significant depth (Ft) | Normal pressure (psi) | Eaton's estimated overpressure (psi) | Bowers Estimated overpressure (psi) | Bowers unloading overpressure (psi) |
|---|---|---|---|---|
| 7600 | 3297.3 | 4121.6 | 4189.2 | - |
| 7700 | 3310.8 | 4395.9 | 4472.9 | - |
| 7800 | 3364.8 | 4594.6 | 4662.2 | - |
| 7900 | 3432.4 | 4837.8 | 4938.4 | - |
| 8000 | 3540.5 | 5189.2 | 5270.3 | - |
| 8100 | 3527 | 5337.8 | 5391.9 | - |
| 8200 | 3554.1 | 5391.9 | 5472.9 | - |
| 8300 | 3585.1 | 5472.9 | 5540.5 | - |
| 8400 | 3635.1 | 5662.2 | 5743.2 | - |
| 8500 | 3689.2 | 5675.7 | 5747.3 | - |
| 8600 | 3743.2 | 5608.1 | 5675.7 | - |
| 8700 | 3770.2 | 5567.6 | 3648.6 | - |
| 8800 | 3824.3 | 5540.5 | 5581.1 | - |

**Table 5: Overpressure values estimated from Eaton's and Bowers method in overpressure zone B, Unag 001 well (TOV at 9200ft)**

| Significant depth (Ft) | Normal pressure (psi) | Eaton's estimated overpressure (psi) | Bowers Estimated overpressure (psi) | Bowers unloading overpressure (psi) |
|---|---|---|---|---|
| 9200 | 3986.5 | 5405.4 | 5472.9 | - |
| 9300 | 4027 | 5472.9 | 5527 | - |
| 9400 | 4067.6 | 5770.3 | 5810.8 | - |
| 9500 | 4121.6 | 6081.1 | 6148.6 | - |
| 9600 | 4162.2 | 6083.8 | 6216.2 | - |

| | | | | |
|---|---|---|---|---|
| 9700 | 4229.7 | 6175.7 | 6229.7 | - |
| 9800 | 4256.8 | 6149.9 | 6216.2 | - |
| 9900 | 4324.3 | 6145.1 | 6202.7 | - |
| 10000 | 4364.9 | 6094.6 | 6151.4 | - |
| 10100 | 4405.4 | 6094.6 | 6148.6 | - |

**Table 6: Overpressure values estimated from Eaton's and Bowers method in overpressure zone C, Unag-001 well (TOV at 10500ft)**

| Significant depth (ft) | Normal pressure (psi) | Eaton's estimated overpressure (psi) | Bowers Estimated overpressure (psi) | Bowers unloading overpressure (psi) |
|---|---|---|---|---|
| 10500 | 4540 | 7162.2 | 7229.7 | 8162.2 |
| 10600 | 4594.6 | 7432.4 | 7499.9 | 8216.2 |
| 10700 | 4662.2 | 7621.6 | 7702.7 | 8472.9 |
| 10800 | 4716.2 | 7743.2 | 7824.3 | 8540.5 |
| 10900 | 4770.2 | 7810.8 | 7905.4 | 8648.6 |
| 11000 | 4797.3 | 7891.9 | 7972.9 | 8785.8 |

**Table 7: Overpressure values estimated from Eaton's and Bowers method in overpressure zone A, Unag-002 well (TOV at 8100ft)**

| Significant depth (Ft) | Normal Pressure (psi) | Eaton's estimated overpressure (psi) | Bowers Estimated overpressure (psi) | Bowers unloading overpressure (psi) |
|---|---|---|---|---|
| 8100 | 3538 | 3942.3 | 4038.5 | - |
| 8200 | 3367.3 | 4230.8 | 4278.8 | - |
| 8300 | 3605.9 | 4519.2 | 4711.5 | - |
| 8400 | 3644.4 | 4567.3 | 4807.7 | - |
| 8500 | 3653.8 | 4615.4 | 4807.7 | - |

**Table 8: Overpressure values estimated from Eaton's and Bowers method in overpressure zone B, Unag-002 well (TOV at 8700ft)**

| Significant depth registration (Ft) | Normal pressure (psi) | Eaton's estimated overpressure (psi) | Bowers Estimated overpressure (psi) | Bowers unloading overpressure (psi) |
|---|---|---|---|---|
| 8700 | 3750 | 4500 | 4548.1 | - |
| 8800 | 3788.5 | 4423.1 | 4519.2 | - |
| 8900 | 3826.9 | 4625 | 4663.5 | - |
| 9000 | 3884.6 | 5000 | 5048.1 | - |
| 9100 | 3923.1 | 5192.3 | 5288.5 | - |
| 9200 | 3971.2 | 4711.5 | 4903.9 | - |
| 9300 | 3971.2 | 4915.4 | 5000 | - |
| 9400 | 4048.1 | 4998.1 | 5049 | - |
| 9500 | 4096.2 | 5192.3 | 5240.4 | - |
| 9600 | 4134.6 | 5028.7 | 5050.9 | - |
| 9700 | 4182.7 | 5480.8 | 5528.8 | - |

**Table 9: Overpressure values estimated from Eaton's and Bowers method in overpressure zone C, Unag-002 well (TOV at 10300ft)**

| Significant depth (ft.) | Normal pressure (psi) | Eaton's estimated overpressure (psi) | Bowers Estimated overpressure (psi) | Bowers unloading overpressure (psi) |
|---|---|---|---|---|
| 10300 | 4451.9 | 5673.1 | 5676.6 | - |
| 10400 | 4500 | 6355.8 | 6346.2 | - |
| 10500 | 4548.1 | 5961 | 5942.3 | - |
| 10600 | 4586.6 | 5673.1 | 5579.9 | - |
| 10700 | 4615.4 | 5663.5 | 5557.7 | - |
| 10800 | 4663.5 | 5965.4 | 5971.2 | - |
| 10900 | 4711.5 | 6057.8 | 5865.4 | - |
| 11000 | 4758.6 | 6923.1 | 6826.9 | - |

**Table 10: Overpressure values estimated from Eaton's and Bowers method in overpressure zone A, Unag-003 well (TOV at 8000ft)**

| Significant depth registration (ft.) | Normal Pressure (psi) | Eaton's estimated overpressure (psi) | Bowers Estimated overpressure (psi) | Bowers unloading overpressure (psi) |
|---|---|---|---|---|
| 8000 | 3455.9 | 3576.5 | 3676.5 | - |
| 8100 | 3529.4 | 3695 | 3823.5 | - |
| 8200 | 3573.5 | 4117.6 | 4147 | - |
| 8300 | 3647.1 | 4411.8 | 4470.6 | - |
| 8400 | 3676.5 | 4264.7 | 4308.8 | - |
| 8500 | 3705.9 | 4382.3 | 4411.8 | - |
| 8600 | 3749.9 | 4558.8 | 4573.5 | - |
| 8700 | 3794.1 | 4411.8 | 4455.9 | - |
| 8800 | 3838.2 | 4485.3 | 4544.1 | - |
| 8900 | 3897.1 | 4705.9 | 4779.4 | - |
| 9000 | 3941.2 | 4044.1 | 4117.6 | - |

**Table 11: Overpressure values estimated from Eaton's and Bowers method in overpressure zone B, Unag-003 well (TOV at 10,000ft)**

| Significant depth In (Ft) | Normal Pressure (psi) | Eaton's estimated overpressure (psi) | Bowers Estimated overpressure (psi) | Bowers unloading overpressure (psi) |
|---|---|---|---|---|
| 10000 | 4294.1 | 5102.9 | 5338.2 | - |
| 10100 | 4323.5 | 5073.5 | 5235.3 | - |
| 10200 | 4411.8 | 5279.4 | 5294.1 | - |
| 10300 | 4470.6 | 5367.6 | 5632.3 | - |
| 10400 | 4518.7 | 5808.8 | 6220.6 | - |
| 10500 | 4558.8 | 5882.3 | 6323.5 | - |

**Table 12: Overpressure values estimated from Eaton's and Bowers method in overpressure zone C, Una- 003 well (TOV at 11800ft)**

| Significant depth (ft) | Normal Pressure (psi) | Eaton's estimated overpressure (psi) | Bowers Estimated overpressure (psi) | Bowers unloading overpressure (psi) |
|---|---|---|---|---|
| 11800 | 5147.1 | 6470.6 | 6176.5 | - |
| 11900 | 5205.9 | 6617.6 | 6323.5 | - |
| 12000 | 5264.7 | 7794.1 | 7205.8 | 7500.3 |
| 12100 | 5279.4 | 8088.2 | 7352.9 | 7647.1 |
| 12200 | 5352.9 | 8529.4 | 7779.4 | 7838.2 |
| 12300 | 5382.4 | 8676.5 | 7926.5 | 8220.6 |
| 12400 | 5411.8 | 8382.3 | 7794.1 | 8352.9 |
| 12500 | 5429.5 | 8235.3 | 7500.1 | 8485.3 |
| 12600 | 5441.2 | 8088.3 | 7514.7 | 8602.9 |
| 12700 | 5470.6 | 8117.6 | 7470.6 | 8661.8 |

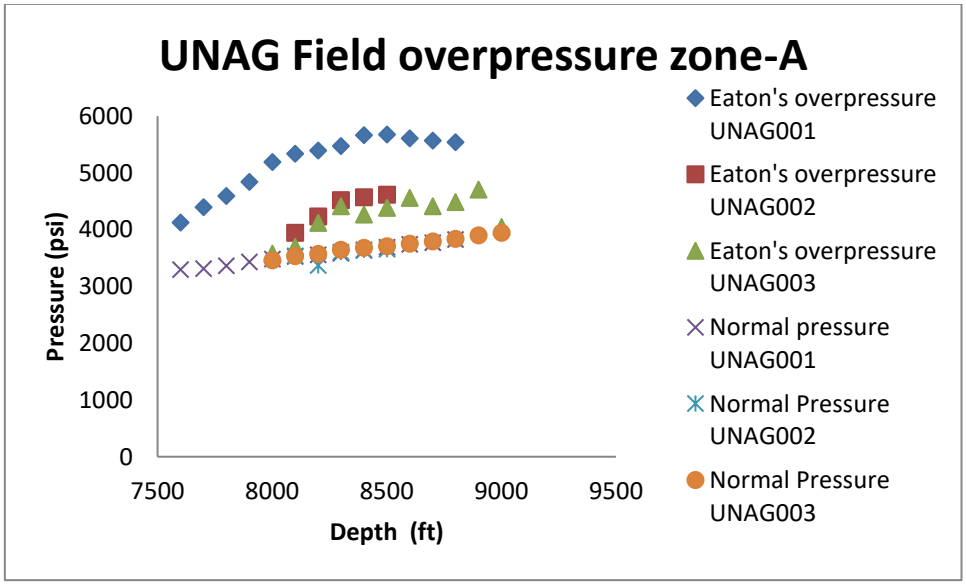

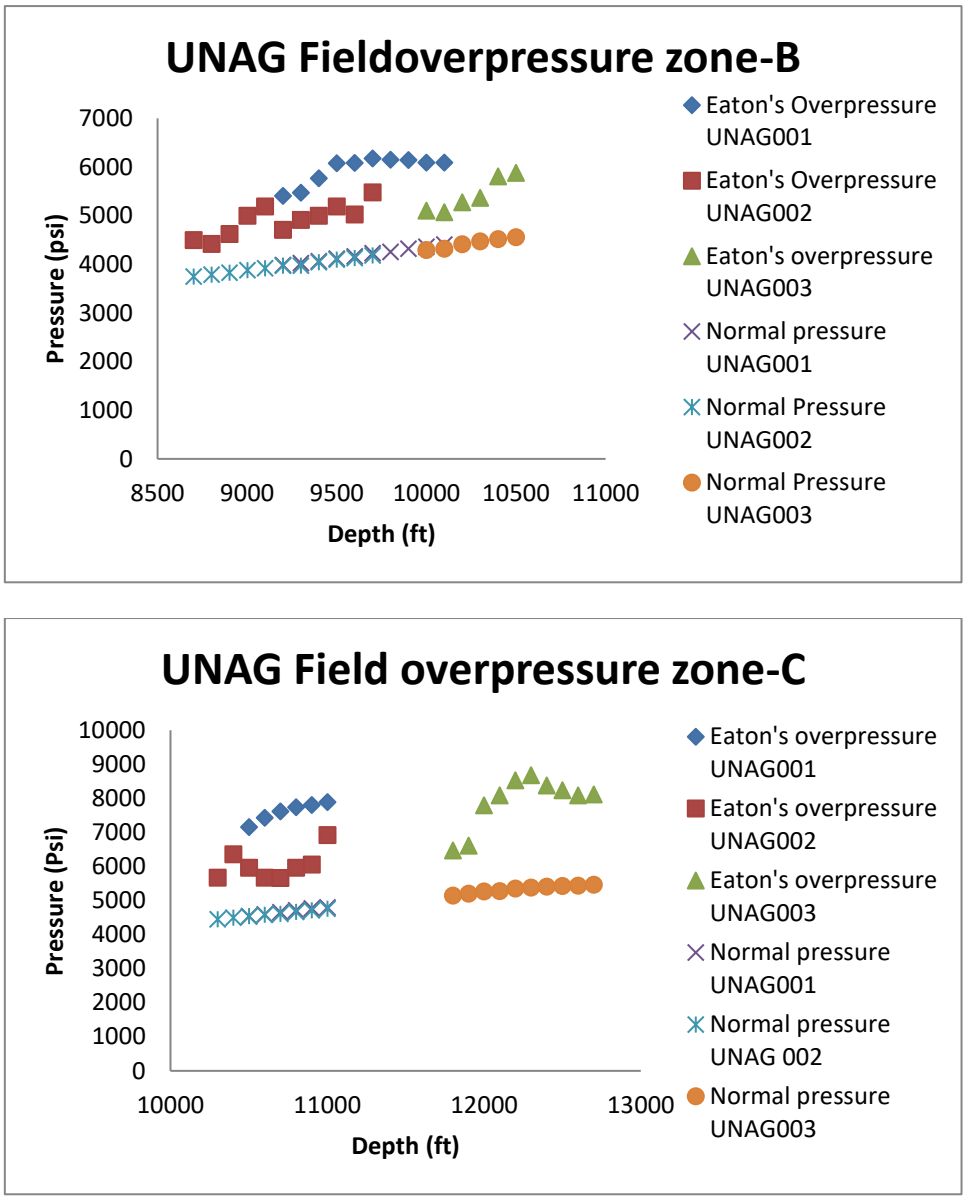


**Fig 5.** Chart showing Overpressure zones across the three wells in UNAG field from Eaton's empirical model

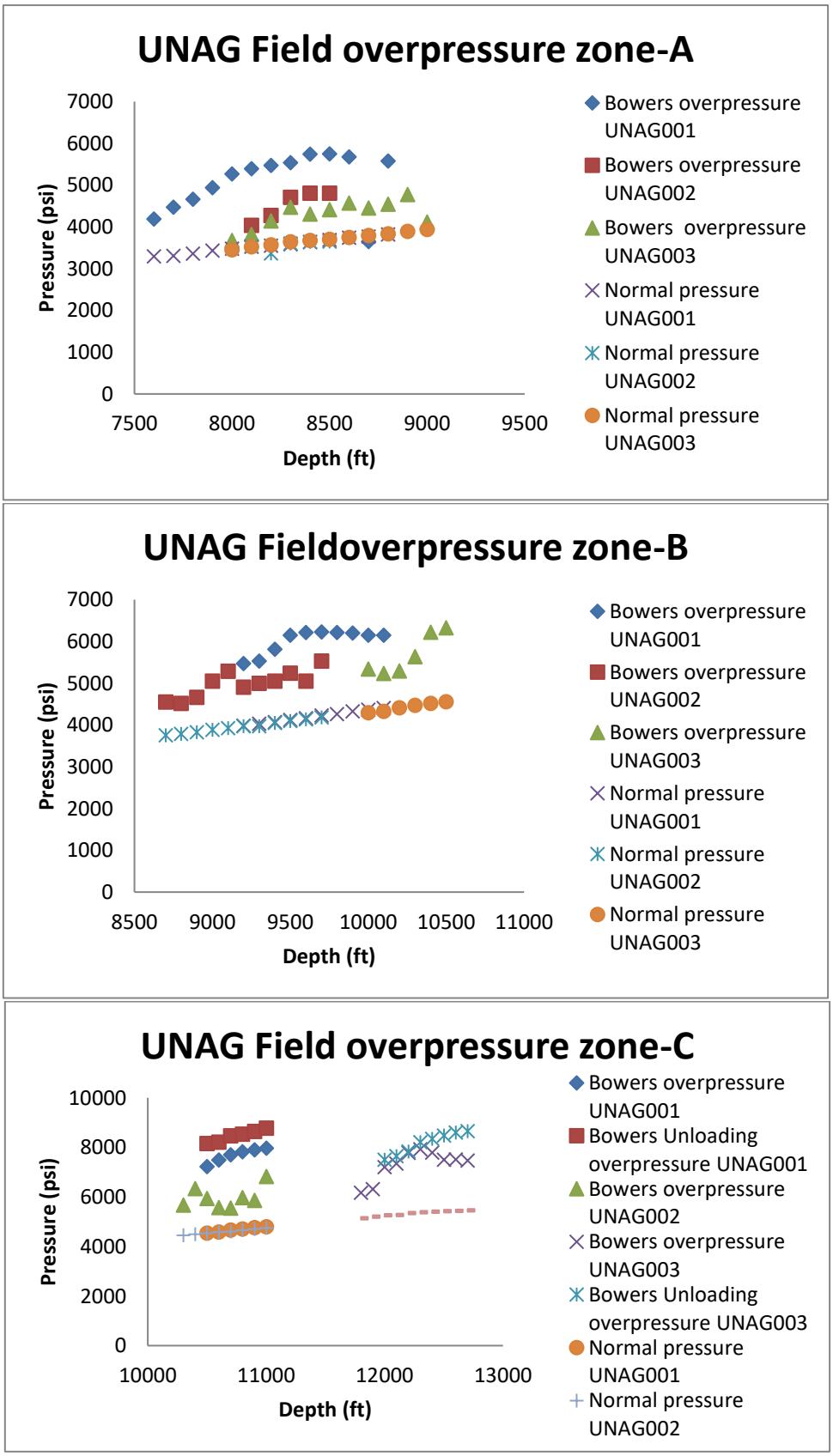


**Fig 6.** Chart showing Overpressure zones across the three wells in UNAG field from Bowers' empirical model

**Table 13: Summary of overpressure play in UNAG-Field**

| WELLS | SIGNIFICANT DEPTH (Ft) | DEPTH OF OVERPRESSURE ENCOUNTERED | AVERAGE EATON'S OVERPRESSURE (PSI) | AVERAGE BOWERS OVERPRESSURE (PSI) |
|---|---|---|---|---|
| **UNAG-001** | 6000 – 11500 | 7600 – 8800; 9200 – 10100; | 5184.29 | 5102.63 |
| | | 10500 – 11000 | 5947.34 | 6012.41 |
| | | | 7610.35 | 8471.03 |
| **UNAG-002** | 4000– 11500 | 8100 – 8500; 8700 – 9700; 10300 – 11000 | 4375 | 4528.84 |
| | | | 4748.08 | 4813.48 |
| | | | 5915.75 | 5886.25 |
| **UNAG-003** | 5000 – 12000 | 8000 – 9000;10000– 10500; 11800– 12700 | 4241.25 | 4300.79 |
| | | | 5419.08 | 5674 |
| | | | 7899.99 | 8163.63 |

## Discussion

From the results presented above, while Eaton's method is proficient in overpressure determination and estimation, Bowers' method is prominent in accounting for unloading overpressure. Three overpressure zones tagged A, B and C have been identified across the three wells, and the tops of these overpressure zones occurred at relatively similar depths laterally across the wells. Velocity reversals from normal compaction trends in velocity logs and a significant increase of pore pressue away from the normal or hydrostatic pressure from Eaton's and Bowers' models were used to identify the top of these overpressure zones.

Normal pressure increases with depth and any pressure that exceeds normal pressure is deemed to be overpressure. Sequel to this, overpressures from all three overpressure zones alongside its constituent normal pressure were plotted against depth to delineate a schematic representation of the actual difference of each overpressure reading away from their normal pressure equivalent, see Figures 3, 4 5 and 6. Shales are more responsive to overpressure due to compaction because they contain clay minerals that can easily be compressed, thus overpressure analysis has been centered on shale lithology in this research. In the presence of a sandy shale zone lithology, overpressure readings may tend to be high because sand is more porous due to its mineralogical composition when compared to a clean shale zone.

The pressure patterns in overpressure Zone A appear to have followed the same curve, thus, suggesting an anticlinal structure. Moreover, if we trace the depths at which the top of overpressure was picked across the wells on the lithologic logs in the 2D Empirical models in Figures 3 and 4, a visible thick succession of shale in UNAG-001 can be seen, however, the shale layers appears to be pinching out from UNAG-002 and 003 wells respectively, thus, the wells may have been drilled across an anticlinal structure that appears to be pinching out downdip.

UNAG-001 well has been associated with more overpressure play compared to the rest wells because it has more extensive clean shale succession and a larger vertical extent of overpressure depth in all the overpressure zones combined. In addition, it also has the highest mean overpressure reading in all the overpressure zone except for overpressure zone C. The estimated overpressure magnitude from Eaton's and Bowers' empirical model has been identified to have similar values downdip, except for depths associated with unloading, see Tables 3 – 9. The

least over pressured well in the study area is UNAG 002, followed by UNAG 003 and UNAG 001. Overpressure zones A and C have been identified to have the highest pressure magnitude because they have more clean shale succession and has been associated with unloading event, moreover, the latter has the highest average overpressure magnitude. Pressure play in UNAG 002 has been minimal due to the presence of more successions of sandstone as exposed from the lithologic log in Figure 3.

In many tertiary sedimentary basins around the world, it may likely be possible that loading events of under compaction are the primary cause of overpressure and at the precipice of these events, secondary overpressure mechanisms of unloading may occur (Chopra and Huffman, 2006). Overpressure from under compaction increases steadily with depth until it reaches zones of unloading mechanism where the overpressure may increase exponentially. In this research, pressure readings in overpressure zones A and C has increased steadily as depth increase, but at deeper depths where overpressure zone C is located, it has been observed that the pressure magnitude increased rapidly from the normal overpressure incremental trend.

## V. CONCLUSION

Overpressure studies carried out on UNAG offshore field is centered on shale lithology, because shales are more responsive to compaction than sandstones. From this study, it is established that UNAG offshore field has been associated with overpressure and this overpressure has been majorly detected on shale layers in the Agbada formation of the field. The layers on which overpressure was detected has been subcategorized into zones namely, A, B and C. The aforementioned overpressure zones have been picked according to their depth of occurrence from shallow to deep. The top of overpressure in these zones varies across the well. Loading mechanism of under-compaction has been majorly responsible for the pressure build in this field, however, deeper depths exhibited massive pressure upsurge which may be due to the presence of unloading effects of overpressure mechanism. Overpressure magnitude is highest in overpressure zone C across the well followed by A and B. While UNAG-001 has been drilled across more hard overpressured succession of layers, UNAG-002 has encountered the least overpressure magnitudes across the pressure zones.

### Recommendation

From the results of this study the following considerations are recommended: the overpressure zones identified pose a significant risk to the drilling process, therefore, drilling of these zones requires the use of special drilling designs. Secondly, provision of pressure data such as repeat formation tester (RFT) tool which measures formation pressure quickly and accurately at specific intervals in the well, to improve overpressure detection and interpretation.

## REFERENCES

[1]. Nwaufa W.A., Horsfall D.E., Ojo C.A. (2006). Advances in deep drilling in the Niger Delta, 1970–2000. In: NAOC experience, NAPE conference proceedings, August 2006, pp 5–14.
[2]. Bowers, G. L., (2002). Pressure Regimes in Sedimentary Basins and Their Prediction, *AAPG* Memoir 76: 217-233.
[3]. Chopra, S. And Huffman, A., (2006). Velocity determination for pore pressure prediction, *CSEG recorder*, p.28-31.
[4]. Dutta, N., (2002). Geopressure prediction using seismic data: current status and the road ahead, Geophysics, 67(6), p 2012-2041.
[5]. Unuagba, T., Ideozu, R. U., Eze, S., Osung, E., & Abolarin, O. (2021). Prediction of Overpressure using Effective Stress and Velocity Trend Methods in Unag field Offshore Niger Delta, Int'l Journal of Research and Innovation in Applied Science (IJRIAS), Vol. VI, Issue I, p. 134-145.
[6]. Terzaghi, K., (1943). Theoretical Soil Mechanics. J Wiley and Sons, Inc., University of Michigan, USA.
[7]. Eaton, B. A., (1975). The Equation for Geopressure Prediction from Well Logs. *Society of Petroleum Engineers of AIME.* Paper SPE 5544.

[8]. Bowers, G. L., (1995). Pore pressure estimation from velocity data; accounting for overpressure mechanisms besides under compaction. *SPE* Drilling and Completions, June, 1995, pp. 89–95.
[9]. Doust, H., and Omatsola, E., (1990). Niger Delta, *in*, Edwards, J. D., and Santogrossi, P. A., eds., Divergent/passive Margin Basins, AAPG Memoir 48: Tulsa, *American Association of Petroleum Geologist*s, p. 239-248.
[10]. Kulke, H., (1995). Regional Petroleum Geology of the World. Part II: Africa, America, Australia and Antarctica: Berlin, Gebrüder Borntraeger, p. 143-172.
[11]. Hospers, J., (1965). Gravity field and structure of the Niger Delta, Nigeria, West Africa: *Geological Society of American Bulletin*, v. 76, p. 407-422.
[12]. Kaplan, A., Lusser, C.U., Norton, I.O., (1994). Tectonic map of the world, panel 10: Tulsa, American Association of Petroleum Geologists, scale 1:10,000,000.
[13]. Avbovbo A.A. (1978). Tertiary lithostratigraphy of Niger Delta. Am Assoc Pet Bill 62: 295–300
[14]. Zhang J. (2011). "Pore pressure prediction from well logs: Methods, modifications, and new approaches", Elsevier. Vol.108, ISS.1-2, pp. 50 – 63.